Low-Energy Electron-Induced Damage in Hexadecanethiolate Monolayers

H. U. Müller, M. Zharnikov,* B. Völkel, A. Schertel, P. Harder, and M. Grunze

Angewandte Physikalische Chemie, Universität Heidelberg, Im Neuenheimer Feld 253, D-69120 Heidelberg, Germany

Received: April 16, 1998; In Final Form: June 22, 1998

Low-energy electron-induced damage in hexadecanethiolate (HDT) monolayers on gold substrates has been investigated using infrared reflection−absorption spectroscopy (IRAS), angle-resolved near edge X-ray absorption fine structure spectroscopy (NEXAFS), and advancing water contact angle measurements. HDT films were exposed to electrons of energies 10−100 eV and doses between 30 and 14 000 μC/cm^2. The induced damage was monitored both "in situ" by NEXAFS measurements interleaved with electron irradiations and "ex-situ" by NEXAFS, IRAS, and contact angle measurements after exposure of the irradiated samples to air. A progressive film damage was observed with increasing electron energy and dose of irradiation. This damage was found to occur during irradiation in UHV and was not induced by chemical reactions with airborne molecules during subsequent exposure of the irradiated films to air. The damage starts in the region of the terminal methyl groups of the HDT films and propagates into the bulk of the film. An analysis of the IRAS and NEXAFS data shows that the conformational and orientational order within the HDT film are most sensitive to low-energy electron irradiation. Electron-induced cleavage of C−H and C−C bonds resulting in a partial desorption of the film constituents also occurs and leads to formation of C=C double bonds in the film as inferred from the appearance of a π^*-resonance in the C 1s NEXAFS spectra. The obtained results are of importance for both the optimization of self-assembled-monolayers-based lithography processes and for the general understanding of irradiation-induced changes in organic films.

1. Introduction

An established method for producing nanometer scale structures is based on the patterning of a polymeric resist with an electron beam writer. Due to the electron exposure, the solubility of the polymer is changed, either by bond breaking or by cross-linking. In a subsequent development process the less solvable regions of the resist are rinsed off to obtain a mask for a pattern-transfer step. During this final step the pattern is transferred into the underlying substrate by an etching process. The achievable resolution of this technique is typically determined by the lateral molecular dimensions of the resist constituents. Practically, the thickness of the resist is also of importance, since elastic and inelastic scattering of the primary and secondary electrons within a thick resist layer results in a progressive spread of the primary beam, which increases the effective size of the irradiated area.

A promising class of ultrathin resists are self-assembled monolayers (SAMs).[1] These are organic molecular assemblies that spontaneously form dense and ordered monolayers on an appropriate substrate. SAMs have successfully been deposited on metals such as gold, silver, copper, platinum, and chromium[2−5] and on oxide and semiconductor surfaces such as SiO_2 and GaAs.[1,6,7] Due to their small intermolecular distance of less than 1 nm, the theoretical attainable resolution is extremely high. Also, the typical thickness of a monolayer film of about 2 nm is favorable in terms of avoiding scattering of the primary and secondary electrons within the organic film. High-resolution patterning in SAMs has been demonstrated with various lithographic methods[5,8−14] by employing high-energy (several tens kiloelectronvolts) and low-energy (from several tens to several hundreds electronvolts) electrons. Recently, it was shown that sub-10 nm structures in octadecylsiloxane monolayers on silicon can be created.[15] In most cases the final pattern transfer into the underlying substrate was achieved by a wet chemical processing although some SAMs were used also as a selective mask for reactive ion etching.[11,12] The nature of the beam damage, especially the molecular changes in the irradiated regions, and their relation to the etching selectivity are clearly of technological relevance. Further improvements in resist properties such as higher contrast, higher sensitivity, lower defect density, and a tailored threshold energy depend crucially on the understanding of the beam damage mechanisms. Several detailed studies on this topic have been recently published,[16−20] mainly focusing on octadecylsiloxane SAMs on SiO_2 substrates.

In this report, we describe the damage in hexadecanethiolate [$CH_3(CH_2)_{15}S$] films on Au substrates induced by low-energy electron irradiation ($E \leq 100$ eV). We applied infrared and X-ray absorption spectroscopies to monitor orientational, conformational, and chemical changes within the HDT layer. Additionally, advancing water contact angles were recorded to study the wettability of the surface. It is currently believed that studies of damage based on contact angle wettability, infrared absorption spectroscopy, and X-ray absorption spectroscopy are more sensitive to subtle changes in the SAM as compared to photoelectron spectroscopy investigations.[21] The data were analyzed with special emphasis on the mechanism of electron-induced damage which is the basis for etching selectivity in an aqueous KCN solution.

The hexadecanethiolate (HDT) films used in the present investigation form well-characterized self-assembled monolayers. The chainlike alkanethiolate molecules are bonded to the

* To whom correspondence should be addressed. E-mail o60@ix.urz.uni-heidelberg.de.

S1089-5647(98)01886-0 CCC: $15.00
Published on Web 09/19/1998

substrate via their sulfur headgroup forming an ordered ($\sqrt{3} \times \sqrt{3}$)*R*30° lateral lattice on Au(111) surfaces.[2,22] (There is still a discussion concerning the exact arrangement and bonding of the sulfur atoms,[23,27] but this problem is not important for the present work.) The distance between the molecules is about 0.5 nm, which corresponds to a lateral density of 4.65×10^{14} molecules/cm^2. The alkyl chains anchored by the S headgroup are inclined by an angle of about 35° with respect to the surface normal.[28] Essential advantages of alkanethiolate SAMs and, in particular, HDT films are a high degree of orientational order and a low percentage of conformational gauche defects. Low-energy electron-induced damage in alkanethiolate monolayers was previously investigated with respect to irradiation-induced desorption of H_2,[19] disulfide formation,[29] and an additional irradiation due to secondary electrons.[30]

In the following we will give a brief description of the experimental procedure and setup. The data are presented and preliminary discussed in section 3. An extended analysis of the data is given in section 4. Finally, the results are summarized in section 5, which also gives an outlook for future work.

2. Experimental Section

Hexadecanethiolate monolayers were prepared by immersion of 30 nm thick polycrystalline gold films evaporated on titanium-primed (9 nm) flat glass slides (haemacytometer slides from Menzel, Germany) in ethanolic 1 mmol thiol solution.[31] Hexadecanethiol was obtained from Fluka Chemicals, Buchs, Switzerland. After immersion for 24 h in the thiol solution the samples were carefully rinsed with ethanol (analytical grade).

HDT films were irradiated with electrons of energies between 10 and 100 eV and exposures between 30 and 14 000 μC/cm^2. The induced damage was monitored by Fourier transform infrared reflection−absorption spectroscopy (FTIRAS), angle-resolved near edge X-ray absorption fine structure spectroscopy (NEXAFS), and advancing water contact angle measurements. The measurements were carried out after an exposure of the irradiated samples to air. We also performed NEXAFS experiments directly in the vacuum chamber where the electron irradiation occurred. We will refer to the NEXAFS measurements of the irradiated samples exposed and unexposed to air as "ex situ" and "in situ" (with respect to the electron irradiation) experiments, respectively.

Electron exposure for the "ex situ" measurements was performed in a hydrocarbon-free vacuum chamber at a pressure of approximately 2×10^{-8} mbar via a Leybold flood gun (FG-10/35). The irradiated area was limited to a rectangular field of 1 cm^2 size by a metal aperture. To ensure a uniform illumination, the flood gun was mounted in a distance of about 15 cm from the sample. Homogeneity (uniformity) of the electron beam was visually checked by several test exposures and subsequent pattern transfers into gold substrates. The exposures were done with electron energies of 10, 30, and 100 eV and three different dosages. The selected dose values of 30, 300, and 3000 μC/cm^2 correspond to an average number of 0.4, 4, and 40 electrons per thiol molecule. While the experiments at 30 and 100 eV were carried out at a current density of 1 μA/cm^2, the experiments at 10 eV were performed at a reduced current density of 0.2 μA/cm^2 due to limitations of the flood gun.

The electron exposure for the "in situ" measurements was carried out under UHV conditions in a multitechnique analysis chamber[32] via a specially designed low-energy flood gun. The same metal aperture and the same flood gun−sample distance as for the "ex situ" experiments were used. Homogeneity of the electron beam was controlled by special measurements of the sample current profile in the plane perpendicular to the direction of the electron beam. Exposures with electron energies of 10 and 20 eV varied from 125 to 14 000 μC/cm^2 (1.7−190 electrons per thiol molecule) and from 140 to 2800 μC/cm^2 (1.9−38 electrons per thiol molecule), respectively. The current densities were 2 and 1.7 μA/cm^2 for the 10 and 20 eV exposures, respectively.

After irradiation the samples ("ex situ" measurements) were transferred through the ambient atmosphere into an infrared spectrometer and analyzed by Fourier transform infrared−reflection absorption spectroscopy (FTIRAS). The FTIRAS spectra were acquired using a Brukker IFS 66v FTIR spectrometer equipped with a Spectra-Tech infrared reflection absorption spectroscopy module. The base pressure of the evacuable spectrometer was 10^{-2} mbar. The resolution was set at $\Delta\bar{\nu} = 4$ cm^{-1}, and the number of scans was at least 500 per spectrum. The measurements were conducted with p-polarized light incident at 80° with respect to the surface normal; the size of illuminated area was approximately 1×0.4 cm^2. To correct for the contribution of the substrate to the IR signal, all spectra were divided by the spectrum of clean gold.

Both the "in situ" and "ex situ" NEXAFS measurements were performed at the synchrotron radiation facility BESSY (Berlin) at the monochromator HE-TGM 2 (high energy toroidal grating monochromator).[33] The energy resolution was better than 0.8 eV at the carbon 1s edge. All spectra were taken in the partial-yield mode with a retarding voltage of −150 V. For selected samples and doses the angle of incidence of the X-ray photons was varied from 90° (the **E** vector in the surface plane: normal incidence) to 20° (the **E** vector near the surface normal: grazing incidence) to monitor orientational order within the HDT films. The resonant photoexcitation process strongly depends on the relative orientation of the light polarization with respect to the vector orbital under consideration. Therefore, the dependence of the intensity of a characteristic NEXAFS resonance on photon incidence angle provides information on the average orientation of the corresponding molecular orbitals in the investigated film.

The raw NEXAFS spectra were normalized to the incident photon flux by division through a spectrum of a clean, freshly sputtered gold sample. For absolute energy calibration the simultaneously measured photoemission current signal of a carbon-covered gold grid with a characteristic resonance at about 285 eV was used. This resonance was separately calibrated by using the NEXAFS spectra of a graphite sample (HOPG); the significant π^* resonance of HOPG was set to 285.38 eV.[34] The size of the synchrotron light spot was approximately 5×1 mm^2 and 10×1 mm^2 at the incidence angles of 90° and 20°, respectively. The acquisition time of every spectrum was about 3 min. All spectra were taken at room temperature. The base pressure in the vacuum chamber during the NEXAFS measurements and electron irradiation ("in situ" experiments) was better than 2×10^{-9} mbar. The transport of the irradiated samples from Heidelberg to BESSY in Berlin ("ex situ" measurements) was performed under a protective argon atmosphere.

Advancing water contact angles were measured with a Krüss goniometer model G 1 under ambient conditions, i.e., at room temperature in a water vapor saturated atmosphere. The reported values were measured on both sides of the drops and are the average of at least three measurements on different surface areas on the samples surface. Deviations from the average values were less than 4°.

The total doses of electron irradiation were estimated by the multiplication of the exposure time by the corresponding sample current corrected for the secondary and backscattered primary electrons emitted from the sample. The correction has been done by division of the sample current by the factor $(1 - \delta)$, where δ is the relative secondary electron yield for both the true secondary and backscattered primary electrons.[30] The uncertainty in the value of δ represents the main disadvantage of this procedure and results in a relatively large error in the dose. We have used a relative secondary electron yield δ of 0.35, 0.42, 0.49, and 0.88 for the 10, 20, 30, and 100 eV primary beam energies, respectively. The values of δ were determined in separate experiments on HDT films on gold.[35] They agree rather well with the literature data for clean gold[36−38] but differ (are smaller) by 10−30% from the recently published results for the HDT/Au system.[30]

Our theoretical estimations following the argumentation of Reimer[39] show that any damage due to a local heating can be ruled out in the range of the current densities used (0.2−2 μC/cm^2). "Ex situ" NEXAFS measurements performed in the current density range of 0.5−1.5 μC/cm^2 ($E = 30$ eV) showed no damage difference for different current densities but equal dose.

3. Results

In this section the results are presented and shortly discussed in four separate parts: (1) infrared absorption spectroscopy data, (2) "ex situ" NEXAFS measurements, (3) "in situ" NEXAFS measurements, and (4) advancing water contact angle data. An extended discussion of the results will be given in section 4.

3.1. Infrared Absorption Spectroscopy. Infrared reflection−absorption spectra were recorded in the C−H stretching region for HDT monolayers on gold. The corresponding spectra for both the HDT samples exposed to the electrons and for the neat reference HDT sample are shown in Figure 1 and Figure 2. Whereas in Figure 1 the dose of irradiation is varied and the energy of electrons is kept constant, data for different energies and a fixed dose of irradiation (3000 μC/cm^2) are presented in Figure 2. The characteristic absorption maxima are indicated in the spectrum for the reference sample; the intensities and positions of these maxima are summarized in Table 1. It is obvious from Figures 1 and 2 and Table 1 that exposure of the monolayers to the electrons resulted in a shift of the peak positions and in changes of peak widths and heights. The changes become more pronounced with increasing dosage and electron energy. The intensities of all C−H modes decrease, and the peaks become broader and shift slightly to higher frequencies in the course of irradiation. Whereas the loss of intensity is apparently due to breaking of C−H bonds, well-known for organic materials from electron microscopy,[39] the latter two effects can stem from disordering of the film: the broadening of the peaks and the blue shift indicate inhomogeneity and reduced molecular order in the film.

A comparison of the CH_3 and CH_2 mode intensities as a function of irradiation dose and electron energy shows that the methyl groups are affected significantly stronger by the irradiation than the methylene groups. Relatively large doses and energies (3000 μC/cm^2, 30−100 eV) are necessary to significantly change the intensities and widths of the CH_2 modes, whereas even gentle electron exposures of the HDT films lead to the pronounced intensity decrease and broadening of the CH_3 modes. This observation suggests that at the first stage of electron irradiation damage occurs predominately in the region of the terminal methyl groups. Both C−H bond dissociation and a change of orientation of the methyl group can result in the observed behavior of the CH_3 absorption modes. The increase of the asymmetric and simultaneous decrease of the symmetric methyl stretch band at a small electron exposure of 30 μC/cm^2 (Figure 1) show that reorientation occurs. In fact,

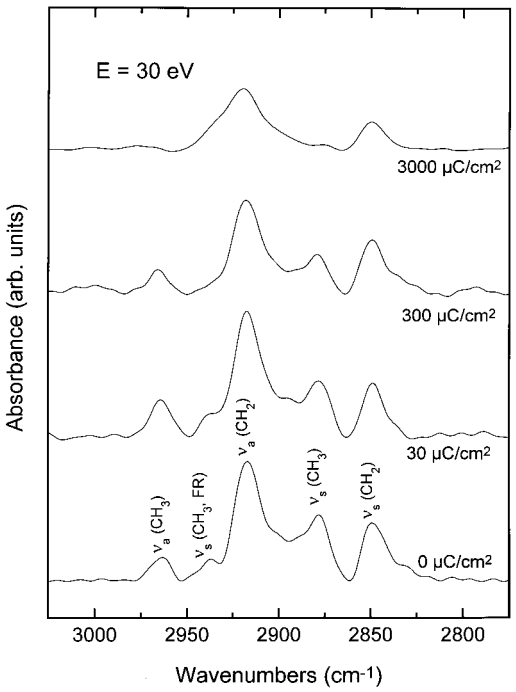

Figure 1. Infrared reflection−absorption spectra for the neat reference HDT film (bottom curve) and HDT films exposed to electrons at a variable dose of irradiation. The primary energy of electrons was constant and equal to 30 eV. The doses are indicated near the corresponding curves. The characteristic absorption maxima are indicated in the spectrum for the reference sample.

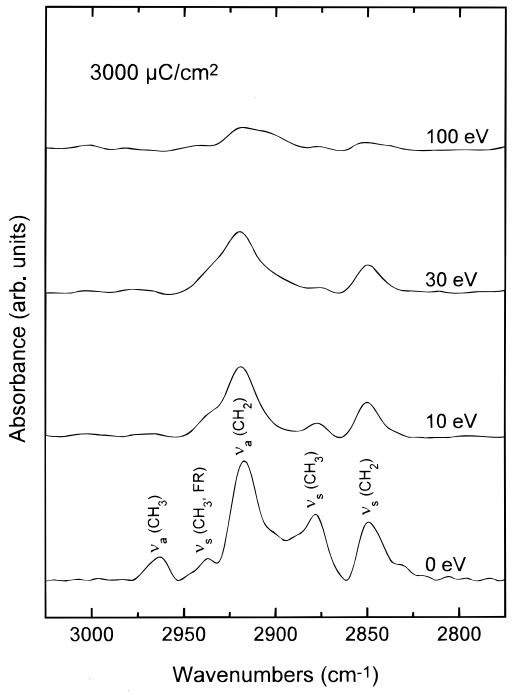

Figure 2. Infrared reflection−absorption spectra for the neat reference HDT sample (bottom curve) and the HDT samples exposed to electrons of different primary energies. The dose of irradiation was constant and equal to 3000 μC/cm^2. The primary energies are indicated near the corresponding curves. The characteristic absorption maxima are indicated in the spectrum for the reference sample.

TABLE 1: IR Absorption Mode Positions [cm^{-1}]/Fwhms [cm^{-1}] for Hexadecanethiolate Films

stretching mode	CH_3, asym	CH_3, sym FR	CH_2, asym	CH_3, sym	CH_2, sym
HDT, reference	2964/12	2938/10	2917/15	2878/13	2849/15
HDT, irradiated energy/dosage					
10 eV/3000 μC/cm^2	x	x	2919/24	2877/11	2850/14
30 eV/3000 μC/cm^2	x	x	2920/29	x	2850/15
100 eV/3000 μC/cm^2	x	x	2920/29	x	2851/22
30 eV/30 μC/cm^2	2964/13	x	2917/16	2878/13	2849/13
30 eV/300 μC/cm^2	2966/12	x	2918/17	2879/12	2849/16
30 eV/3000 μC/cm^2	x	x	2920/29	x	2850/15

[a] x = peak position cannot be determined.

the pronounced symmetric CH_3 mode for the reference HDT sample reveals a strong component of the corresponding transition dipole moment in the normal direction typical for well-ordered alkanethiolate film. A relative change of intensity of this mode with respect to the antisymmetric CH_3 mode implies a reorientation or a loss of the orientational order of methyl groups. Hence, even gentle irradiation of HDT films with electrons results in orientational modifications of the terminal CH_3 groups of the alkyl chains, i.e., in a partial replacement of all-trans conformation of the upper CH_2 entities by gauche conformation. IR spectra simulations for octadecanethiolate on gold by Laibinis et al.[40] give the same (as presented in Figure 1) development of the intensities of the two characteristic methyl modes for the presence of gauche conformation at the topmost CH_2 group. Even if a irradiation-induced loss of intensity of the antisymmetric CH_3 mode occurs at a small electron exposure, it is overcompensated by the gain of intensity due to the reorientation of the CH_3 entities.

3.2. "Ex Situ" NEXAFS measurements. NEXAFS spectroscopy provides information complementary to the infrared absorption spectroscopy data. In the present case NEXAFS spectroscopy has been used to probe transitions of carbon 1s electrons into the lowest unoccupied molecular orbitals (LUMOs) of HDT. Since these antibonding states are spatially directed and related to the specific chemical bonds between the molecular constituents, NEXAFS spectroscopy is sensitive to both the nature of the chemical bonds and to the orientation of the HDT molecules. To distinguish between irradiation-induced changes in chemical bonds and orientational order within the film, NEXAFS measurements were performed at the magic X-ray incident angle of 55° (54.7°). For this particular orientation of the sample with respect to the incident X-rays, the intensity distribution measured in a NEXAFS spectrum is indistinguishable from that for a random molecular orientation and is therefore not sensitive to the orientational order within the object of investigation.[41]

In the left panels of Figures 3 and 4 NEXAFS spectra of hexadecanethiolate films exposed to electrons are displayed (solid lines) together with the spectrum (dashed lines) of the neat reference HDT sample. The differences of the former and the latter NEXAFS spectra are displayed in the right panels of these figures. All presented spectra were recorded at an X-ray incident angle of 55°. In Figure 3 the dose of irradiation is varied at constant electron energy of 30 eV. Data for different energies and a fixed dose of irradiation (3000 μC/cm^2) are presented in Figure 4. Three characteristic resonances are clearly visible in the spectrum of the reference sample, namely, a sharp resonance at ≈287.7 eV, a C−C* resonance at 293.4 eV, and a C−C′ resonance at 301.6 eV above the ionization edge. The transition moments of the molecular orbitals corresponding to the two latter resonances are directed along the alkyl chain axis.

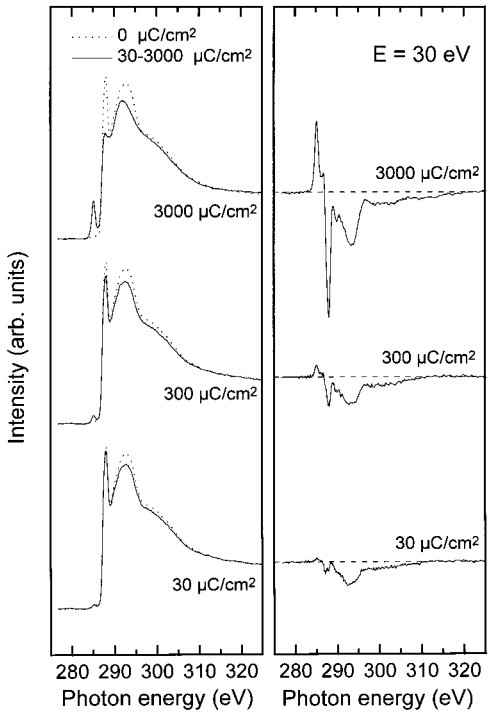

Figure 3. NEXAFS spectra recorded at an X-ray incident angle of 55° for the neat reference HDT film (dashed lines) and HDT films exposed to electrons (solid lines) at a variable dose of irradiation (left panel). The difference spectra (scaled by a factor of 2) with respect to the reference film are shown in the right panel. The primary energy of electrons was constant and equal to 30 eV. The doses are indicated near the corresponding curves.

The exact assignment of the resonance at ≈287.7 eV is somewhat unclear at present. A detailed theoretical analysis[42] implies that this resonance corresponds to the transitions of the C 1s electrons into Rydberg states below the ionization edge. There should be two such transitions into R_σ and R_π orbitals at 287.4 and 288.1 eV, respectively,[42] which cannot be resolved with the energy resolution in our experiments. Both orbitals are spatially extended and oriented perpendicular to the molecular axis of the HDT chains, with the transition dipole moment (TDM) of the R_σ orbital located in the C−C−C plane and the TDM of the R_π orbital perpendicular to this plane. Some questions about this assignment, however, are still discussed. The R* assignment[42] is based on a calculation of an isolated small propane (C_3H_8) molecule, and it is not clear whether the same assignment is correct for the significantly longer alkanethiol molecules. Moreover, a Rydberg resonance should be quenched in a density-packed alkanethiolate SAM film. It is, however, well-known that the resonance at ≈287.7 eV is characteristic for the presence of methylene groups and should be therefore affected by configurational and chemical changes involving these entities. Considering all these circumstances, we will refer to this resonance as a C−H*/R* resonance.

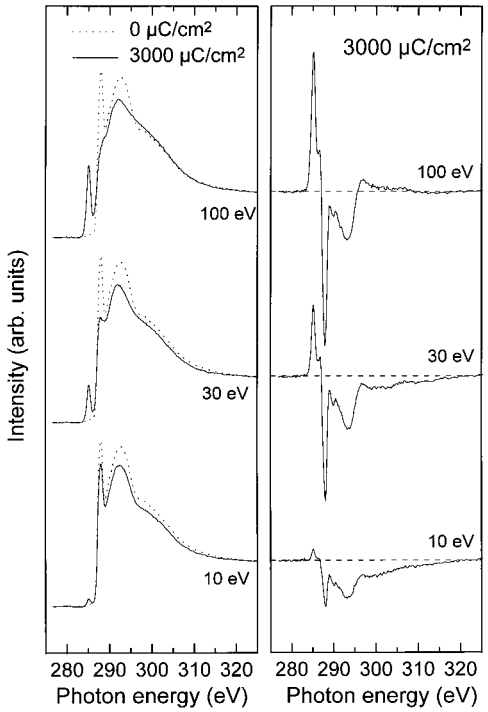

Figure 4. NEXAFS spectra recorded at an X-ray incident angle of 55° for the neat reference HDT film (dashed lines) and HDT films exposed to electrons (solid lines) of different primary energies (left panel). The difference spectra (scaled by a factor of 2) with respect to the reference film are shown in the right panel. The dose of irradiation was constant and equal to 3000 μC/cm^2. The primary energies of electrons are indicated near the corresponding curves.

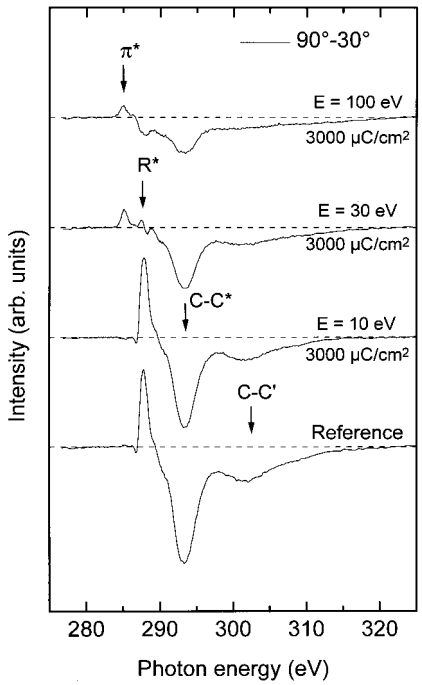

Figure 5. Differences of NEXAFS spectra recorded at X-ray incident angles of 90° and 30° for the neat reference HDT film (bottom curve) and HDT films exposed to electrons of different primary energies. The dose of irradiation was constant and equal to 3000 μC/cm^2. The primary energies of electrons are indicated near the corresponding curves.

The electron bombardment results in significant changes in the NEXAFS spectra (solid lines in Figures 3 and 4). The intensities of the C−C*/C−C′ resonances and especially that of the C−H*/R* resonance decrease, and a new resonance at 285.1 eV characteristic for the C═C double bonds (π* resonance) appears. As observed in infrared absorption spectroscopy, the damage effects become stronger as the dosage or/and the electron energy increases.

The high sensitivity of the C−H*/R* resonance to electron irradiation stems presumably from the fact that its intensity strongly depends on the length of the intact C−H chain (see e.g. ref 28). The creation of defects along the chains such as gauche defects or dissociation of C−H bond destroys the molecular conformation and subsequently results in a significant reduction of the C−H*/R* resonance. Note that molecular orbitals with strong Rydberg character are rather large and thus sensitive to conformational changes. A comparable reduction of the C−H*/R* peak was also observed at heating of alkanethiolate films which was interpreted as indication of creation of conformational disorder of the alkyl chains caused by the development of gauche defects.[43]

The appearance of the π* resonance was, however, not observed in the heating experiments, which means that this resonance is not related to conformational disorder within the alkanethiolate films. The appearance of the π* resonance can be associated with the dissociation of C−H bonds and the subsequent formation of intra- or intermolecular C═C double bonds, which (together with the conformational changes) also affect the intensity of the C−H*/R* resonance. In addition to the π* resonance, two small features appear at 286.7 and 289.9 eV after electron beam exposure. While the increase of intensity at 286.7 eV can be attributed to gauche conformations,[43] the reason for the dip at 289.9 eV is not known.

Besides the NEXAFS measurements at the magic incidence angle, angular dependent NEXAFS experiments were performed to monitor an orientational order within the HDT films. The analysis[44] of the data for the reference HDT film results in an average alkyl chains tilt angle of 35.3° with respect to the substrate normal. This value is in good agreement with previous FTIR[45] and NEXAFS[46] results.

As a fingerprint of an orientational order within the film, the difference of the spectra acquired at normal and grazing incidence can be taken. At normal incidence the **E** vector of the incoming light lies in the surface plane and molecular orbitals with a TDM having a large component along this plane are predominately probed. At grazing incidence the similar situation occurs for the molecular orbitals directed along the surface normal. Therefore, any predominate orientation of some specific vector orbitals within the investigated object will reveal itself as a positive or negative peak in the difference curve. In the case of the HDT film peaks of opposite signs can be expected for the C−H*/R* and the C−C*-/C−C′ resonances in the difference spectra because TDMs of the corresponding molecular orbitals are oriented perpendicular to each other.

In Figure 5 a series of angular difference spectra (90°−30°) for both the reference HDT film and the films exposed to electrons of different energies are reproduced. In agreement with the assumed orientation of the HDT molecules (the mean tilt angle of 35.3°), positive and a negative anisotropy peaks are observed for the C−H*/R* and the C−C*/C−C′ resonances, respectively. The relative high intensity of the anisotropy peaks in the spectrum of the neat film points to a high degree of orientational order. The spectra for the irradiated films indicate a significant loss of orientational order after exposure. Except for the 10 eV curve, the anisotropy peaks corresponding to the C−H*/R* and the C−C*/C−C′ resonances are greatly reduced in intensity, becoming more pronounced with increasing electron energy. The new small anisotropy peak at 285.0 eV observed in the 30 and 100 eV curves indicates a preferred orientation

of the C═C double bonds normal to the substrate surface. (π orbitals are directed perpendicular to the bond direction.) This leads to the conclusion that in these experiments predominately intramolecular double bonds were formed along the alkyl chains (allyl groups $-CH_2-CH=CH_2$) rather than between the adjacent chain molecules.

From the raw NEXAFS data also an effective HDT film thickness can be estimated[46,47] by comparing the intensity before the carbon absorption edge to the intensity of the edge itself. The estimation is based on the assumption that the signal at energies lower than the absorption edge stems only from substrate electrons and that the signal corresponding to the C 1s edge is due to the HDT adsorbate and self-attenuated. These assumptions are largely justified as in the relevant energy range the absorption cross section of gold is about 50 times higher than the cross section of an alkanethiol molecule.[41] However, the extent to which elastically and inelastically scattered electrons contribute to the signal can only be approximated. The estimations show that no pronounced change in thickness is observed after bombardment with 10 eV electrons, while an exposure with higher energies leads to a thickness reduction of 6 and 9% for 30 and 100 eV electrons, respectively (3000 μC/cm^2).

3.3. "In Situ" NEXAFS Measurements. The NEXAFS data presented in section 3.2 clearly demonstrate the main effects of electron-induced damage in the HDT monolayers on gold. However, the rather limited number of samples we were able to study by NEXAFS in the given time and the necessity to transport the differently irradiated samples to BESSY did not allow us to monitor the development of the damage in detail.

Moreover, one of the most important questions, namely, whether the observed damage is a direct result of radiation exposure or is induced by some chemical reactions with air constituents during the subsequent exposure of the irradiated films to air, needs to be addressed. In view of these facts "in situ" NEXAFS measurements without an exposure of irradiated samples to air have been performed. An emphasis was given to the dose variation, whereas the energy of electrons was limited to 10 and 20 eV. These energies were chosen for our first "in situ" experiments presented here because of the relatively moderate damage expected at low energies (which simplifies monitoring of the damage) and the relevance of this energy range for the estimation of the damage produced by secondary electrons.

In the left panel of Figure 6 NEXAFS spectra of hexadecanethiol films exposed to electrons of 10 eV energy are shown together with the spectrum of the neat reference HDT sample. The difference spectra with respect to the neat film are displayed in the right panel of Figure 6. All presented spectra were recorded at an X-ray incident angle of 55°. The spectra and difference curves in Figure 6 demonstrate qualitatively the same development of the damage with increasing dose as was observed in Figure 3 for 30 eV electrons. In the course of irradiation the intensities of the C−C*, C−C′, and especially C−H*/R* resonances decrease, while the new π* resonance appears and develops. The intensities of the C−H*/R* and π* resonances were extracted from the corresponding NEXAFS spectra in Figure 6. These values are plotted in the upper and middle panels of Figure 7 (full quadrates) as a function of the irradiation dose. In the lower panel of Figure 7 the effective thickness of the HDT film estimated from the raw "in situ" NEXAFS spectra is presented. Together with the data for the primary electron energy of 10 eV the data corresponding to the electrons with kinetic energy of 20 eV (full circles; the spectra

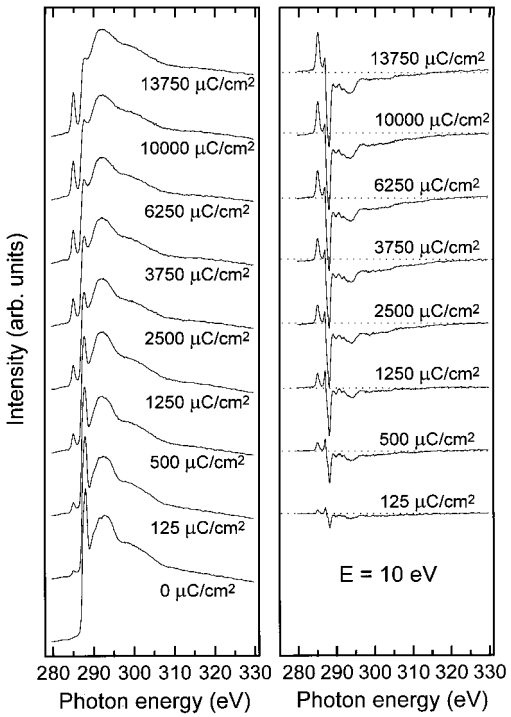

Figure 6. "In situ" NEXAFS spectra recorded at an X-ray incident angle of 55° for the neat reference HDT film (bottom curve) and HDT films exposed to electrons at a variable dose of irradiation (left panel). The difference spectra with respect to the reference film are shown in the right panel. The primary energy of electrons was constant and equal to 10 eV. The doses are indicated near the corresponding curves.

are not shown) are displayed. A comparison of the intensity vs dosage dependencies for the C−H*/R* and π* resonances shows that the intensity of the former resonance decreases rapidly with increasing dose as compared to a rise of intensity of the latter resonance. The high sensitivity of the C−H*/R* resonance to electron irradiation was addressed in the previous section. Both conformational defects and cleavage of C−H/C−C bonds resulting in a partial desorption of the film constituents cause a decrease in resonance intensity. Bond cleavage seems to occur comparatively slow in the course of irradiation as indicated by the slow changes in the π* and C−C resonances as compared to the rapid decrease of the C−H*/R* resonance.

The effective thickness of the HDT film behaves in the same manner as the intensity of the C−H*/R* resonance. This implies that a reduction of the effective thickness is predominately caused by the conformational and orientational changes within the alkanethiolate chains and to a smaller extent by fragmentation and partial desorption of the film. The conformational changes and loss of the orientational order reduce the film thickness but increase the density of the film. Conversion of a thick film with a large mean free path of electrons to a thin, more dense film with a smaller mean free path is at least partially self-compensating but can, in principle, result in a reduction of the effective thickness.

The loss of the orientational order in the HDT occurs also very rapidly with increasing dose of electron irradiation. In Figure 8 series of NEXAFS spectra taken at different angles of incidence for the reference (left panel), moderately irradiated (middle panel), and strongly irradiated (right panel) HDT films are depicted. The corresponding 90°−30° difference spectra are displayed in Figure 9. They show that even a moderate irradiation of the HDT films by electrons results in a very strong reduction of the angular anisotropy of the NEXAFS resonances.

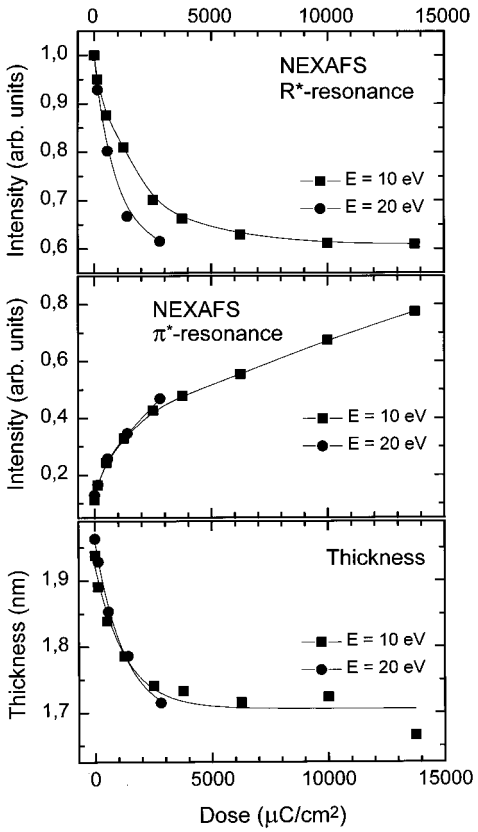

Figure 7. Intensities of the C−H*/R* (upper panel) and π* (middle panel) resonances extracted from the "in situ" NEXAFS spectra recorded at an X-ray incident angle of 55° for the neat reference HDT film and HDT films exposed to electrons as functions of the irradiation dose. In the lower panel the effective thickness of the HDT films estimated from the raw "in situ" NEXAFS spectra is presented as a function of the irradiation dose. The data for the primary electron energies of 10 eV (full quadrates; the corresponding spectra are shown in Figure 6) and 20 eV (full circles; the spectra are not shown in the manuscript) are displayed.

Whereas the characteristic dependence of the NEXAFS spectra for well-ordered alkanethiolate layers on the incidence angle is clearly seen in the left panel of Figure 8, the analogous spectra in the middle panel of Figure 8 exhibit a large resemblance at various angles of incidence. In Figure 9 the corresponding strong reduction of the anisotropy peaks associated with the C−H*/R* and π* resonances is observed. It becomes apparent from both Figure 8 and Figure 9 that further irradiation with low-energy electrons does not affect the remainder of the orientational order significantly; the main effect is produced by moderate doses.

The negative sign of the anisotropy peak assigned to the π* resonance indicates a preferred orientation of the C=C double bonds parallel to the substrate surface. This could indicate that double bonds in the present case are predominately formed between the adjacent chain molecules or that a large concentration of gauche defects reorients the allyl groups. This orientation is different to the "ex situ" NEXAFS results, which could be due to the intermediate air exposure, or to the higher primary energy of electrons used in the "ex situ" experiments (strong irradiation).

Generally, the "in situ" NEXAFS spectra exhibit the same development of absorption peaks with progressive electron irradiation as the "ex situ" NEXAFS spectra. This means that the observed electron-induced damage occurs during irradiation and is not induced by chemical reactions with air constituents during subsequent exposure of the irradiated films to ambiance. This was additionally confirmed by exposure of one of the irradiated samples briefly to air and by comparing the NEXAFS spectra before and after the exposure. The corresponding spectra are depicted in Figure 10, together with the difference spectrum. It can be clearly seen that the spectra before and after exposure to air are practically identical, which means that exposure did not affect the irradiation-induced damage to a noticeable extent. A small increase of the absorption in the energy region of 295−315 eV after air exposure can be related to an adsorption of airborne hydrocarbons on the HDT film during this procedure.

3.4. Advancing Water Contact Angle Measurements. In addition to the knowledge of the irradiation-induced damage on the microscopic scale, an understanding of macroscopic properties of the irradiated HDT films is of a great interest. One of the most important properties is the wetting behavior of the films, because this parameter essentially determines the selectivity and the efficiency of wet etching in a lithography process. In the present case the wetting properties and polarity of the HDT film surface have been probed by measurements of the advancing water contact angle. The dependence of the contact angle on the HDT films on the dose of irradiation is displayed in the upper panel of Figure 11 for three different energies of the primary electron beam. The reference films exhibit a rather large contact angle of 109°, which is usually related to a weak interaction between the terminal CH_3 groups and water molecules.[48] The electron irradiation results in a decrease of the contact angle as a function of increasing dosage or/and electron energy. Gentle irradiation resulting in the appearance of gauche defects in the region of the methyl groups (see section 3.1) leads to a small reduction of the contact angle to a value of about 102°. Such a reduction can be explained by an interaction of water molecules with the CH_2 groups that become exposed to water after the reorientation of the surface methyl groups. In fact, the water contact angle of polyethylene comprising exclusively CH_2 entities is about 102°.[49]

Progressive irradiation of the HDT films results in a further decrease of the contact angle, which can be associated with the appearance of polar groups in the originally methyl-terminated surface layer. Indications of such a process have been observed previously by infrared absorption spectroscopy,[20] where it was suggested that polar COOH groups appear as a result of chemical reactions of the irradiation-created free radicals with oxygen from the ambiance. Analogous reactions with the rest gas constituents within the vacuum chamber can be excluded because of the very low concentration of molecular and atomic oxygen under UHV conditions.

The data displayed in the upper panel of Figure 11 can be presented in a more descriptive form by using energy correction factors to compare the doses for the different primary energies of electrons. These factors can be extracted from the data on the kinetic energy-dependent energy losses of electrons in polyethylene[50] which is very similar to the alkanethiols with respect to atomic density. The correction factors of 0.2, 1, and 3.3 were derived for the primary electron energies of 10, 30, and 100 eV, respectively. The doses for different kinetic energies were then multiplied by these factors in accordance with the value of the energy. The resulting dependence of the water drop contact angle on the equivalent (30 eV) dose of irradiation is depicted in the lower panel of Figure 11. Although some care should be taken in an interpretation of the results, the general tendency given by the curve in the lower panel of Figure 11 is clear. A rather moderate dose of 1500−2000 μC/cm^2 (30 eV) seems to be sufficient for a pronounced reduction of the contact angle, while a further irradiation does not change

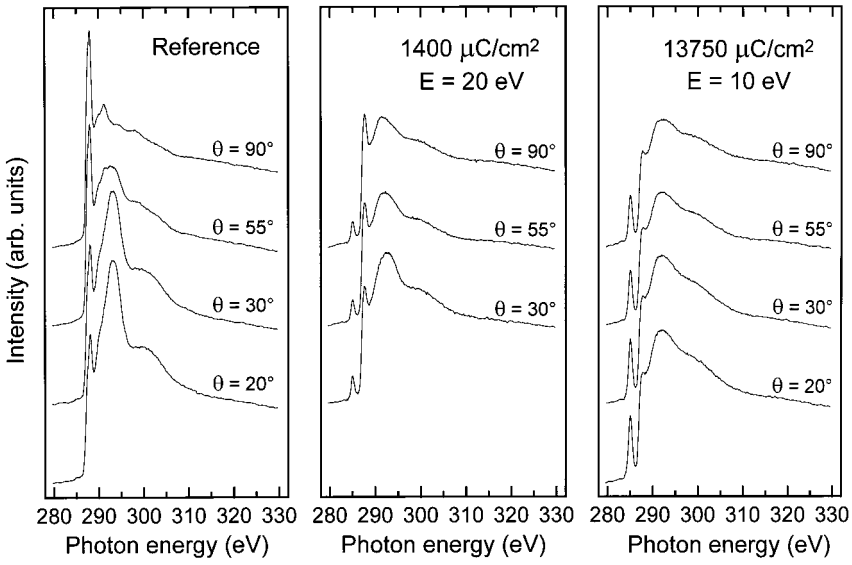

Figure 8. Series of "in situ" NEXAFS spectra at different X-ray incident angles for the reference (left panel), a moderately irradiated (middle panel), and a strongly irradiated (right panel) HDT film. X-ray incident angles are indicated near the corresponding curves.

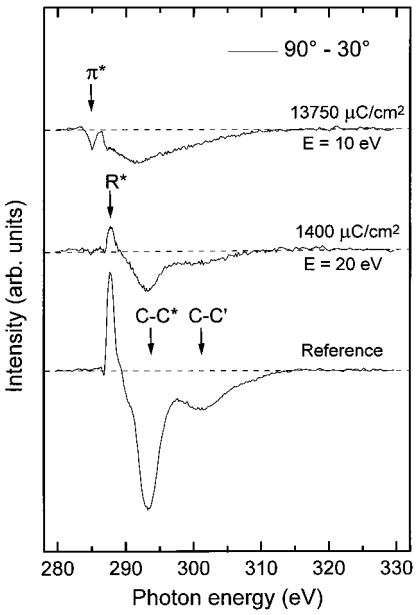

Figure 9. Differences of "in situ" NEXAFS spectra (displayed in Figure 8) recorded at X-ray incident angles of 90° and 30° for the neat reference HDT film (bottom curve) and HDT films exposed to electrons. The doses of irradiation and the primary energies are indicated near the corresponding curves.

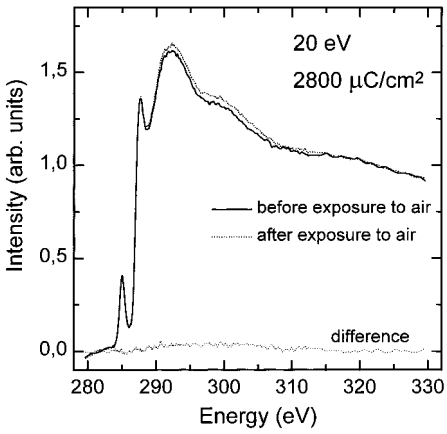

Figure 10. "In situ" NEXAFS spectra for an irradiated HDT film before (solid curve) and after (dotted curve) exposure to air as well as the corresponding difference spectrum (bottom curve).

the contact angle significantly. It can be therefore assumed that irradiation with a dose of 1500−2000 μC/cm^2 at 30 eV results in practically complete damage of the topmost layers of the HDT film, which determine the value of the contact angle.[51] The leveling off of the water contact angle with progressive electron irradiation has been also reported previously for methyl-terminated SAMs[17] and octadecyl derivatives on oxide-covered Si substrates.[20] The ultimate water contact angle of 74°−75° derived from the lower panel of Figure 11 agrees rather well with the corresponding literature values of 60°[17] and 80°.[20]

4. Discussion

Except for some inconsistencies which will be addressed in this section, the results of FTIRAS, "ex situ"/"in situ" NEXAFS, and contact angle measurements give a full and consistent picture of electron irradiation-induced damage in HDT films on gold. A progressive film damage was observed with increasing electron energy and/or dose of irradiation. Damage was found to occur during irradiation and was not induced by chemical reactions with air constituents during subsequent exposure of the irradiated films to air. The damage reveals itself in a decrease of both the water contact angle and the intensities of the characteristic IRAS and NEXAFS resonances typical for a well-ordered system of hydrocarbon chains.

The results of the IRAS and contact angle measurements indicate that at the first stages of electron irradiation electron-induced damage occurs mainly in the region of the terminal methyl groups in the HDT films. Initially, an orientational modification of the terminal CH_3 groups of the alkyl chains, i.e., a partial replacement of all-trans conformation of the upper CH_2 segments by gauche conformation, occurs. With progressive irradiation the damage occurring in the surface region propagates in the bulk of the film. The corresponding development of the NEXAFS C−H*/R* resonance indicates that even a moderate electron irradiation of about 1500−2000 μC/cm^2 (10 eV) results in an almost complete loss of the conformational all-trans order and appearance of structural gauche defects within the HDT chains. This process implies a decrease of orientational order in the film and a reduction of the effective film thickness, which can be also directly derived from the angular dependent

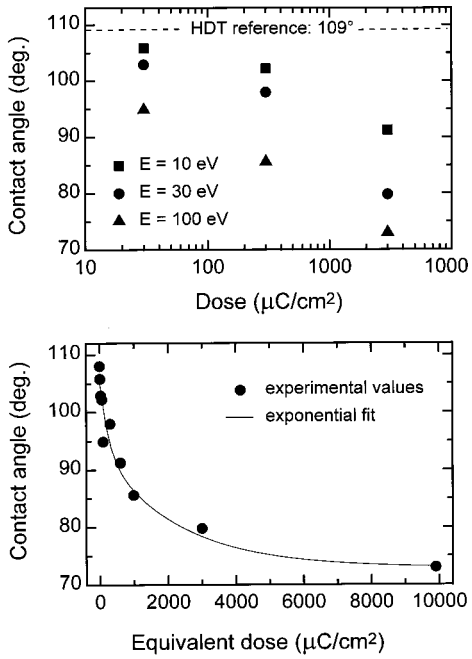

Figure 11. Advancing water contact angles for HDT films after electron irradiation with different energies and doses (upper panel). In the lower panel the dependence of the contact angle on the equivalent (30 eV) dose of irradiation is displayed. To estimate the equivalent doses, the true doses for different kinetic energies were multiplied by special correction factors (see text) in accordance with the value of the primary energy.

NEXAFS measurements and the raw NEXAFS spectra, respectively. Partial desorption of film constituents (and in particular H) may also contribute in the loss of the conformational and orientational order since such a desorption will cause conformational defects. Previous studies have shown that low-energy electron impact (starting at the primary electron energy of ≈7 eV) on alkanethiolate monolayers chemically bound to Au substrates causes desorption of H_2.[19] The loss of hydrogen also results in compacting of the chains to form a reduced thickness, carbonaceous film.[20] Additionally, scission of C−C bonds and a consequent desorption of carbon-containing fragments can occur at low energies, although this process seems to happen at a significantly lower rate than a cleavage of the C−H bonds.[52] The experiments presented in this report do not provide a direct information on the desorption processes. As an indirect measure of a cleavage of the C−H and C−C bonds within the film, which is imperative for subsequent desorption, the intensity of the NEXAFS π^* resonance can be taken. This resonance is associated with the C═C double bond, which is completely absent in the virgin HDT film and appears only as a result of cleavage of C−H and C−C bonds. The NEXAFS data imply that such a cleavage occurs comparatively slowly in the course of electron irradiation than the loss of conformational and orientational orders. The relatively rapid increase of the π^* resonance intensity in the initial stage of irradiation can be associated with the breaking of C−H bonds in the upper part of HDT film. The disagreement of the "ex situ" and "in situ" NEXAFS data concerning a predominate orientation of the formed C═C bonds can be related to the possible influence of a relatively long air exposure preceding the "ex situ" measurements. Therefore, we tend to believe that the results of the "in situ" experiments deserve more trust. Nevertheless, effects connected with the influence of the primary electron energy cannot be completely excluded.

There are also two other discrepancies between "ex situ" and "in situ" NEXAFS experiments. First, the energy dependence of the electron irradiation induced damage is less pronounced in the latter experiments than in the former ones. This inconsistency can be related to the limited energy range for the "in situ" experiments, which did not allow us to make the effects of the primary energy clearly visible.

The second disagreement is a difference of the observed damage for a primary electron energy of 10 eV in the corresponding "ex situ" and "in situ" NEXAFS spectra. At a given dose the former experiments exhibit a smaller irradiation-induced damage than the latter. Although annealing effects in air cannot be excluded, we believe that an uncertainty of the primary energy of electrons in the "ex situ" experiments represents the most probable reason of the considered "contradiction". The electron flood gun used in these experiments is well-suited for the primary energies in the range 50−500 eV but is not especially adequate for the low energies of electrons such as 10 eV. Therefore, the primary electron energy of 10 eV in the "ex situ" experiments could have been smaller than the quoted value, which could explain the smaller apparent damage.

The basic results of the present report are in general comparable with those of previous studies on electron-induced damage in hydrocarbon films, although most of these studies were performed at essentially higher primary electron energies. The effective thickness loss of 10−30% has been observed for strongly (e.g., 300 μC/cm^2 at the primary electron energy of 2 keV[20]) irradiated SAMs on oxidized Si and Ti substrates.[17,18,20] This agrees well with the final value of about 15% obtained in our experiments. The higher values of the effective thickness loss observed in some studies[20] can probably be related to an additional desorption induced by the cumulative impact of high-energy electrons. That the damage levels off in the course of electron irradiation has been observed in general.[17,18,20] This means that irradiation-induced degradation of the film occurs initially fast with increasing electron exposure and then becomes more gradual. We observe qualitatively the same development in the orientational and conformational order, the effective thickness, and the advancing water contact angle of the HDT film. Only the intensity of the NEXAFS π^* resonance related to the cleavage of the C−H and C−C bonds in the HDT film continuously increases with progressive irradiation after the other damage parameters become practically constant. This implies that scission of these bonds by electrons still continues to occur.

Previous studies have assumed that ultimate electron irradiation causes conversion of the SAM to a graphitic material.[17−18] The high resistance of graphite carbon to electron beam irradiation is believed to be the main reason for the "saturation" of damage. The disordered hydrocarbon film obtained in our study in result of the electron irradiation represents a mixture of saturated and unsaturated hydrocarbons as revealed by the occurrence of both C−C* and π^* resonances in the NEXAFS spectra for strongly irradiated HDT films. The characteristic absorption peaks for bulk graphite, namely a π^* resonance at 285.4 eV and a relatively sharp σ^* resonance at 292.5 eV,[34] are not observed in our data. Therefore, formation of graphitic structures seems to be unlikely at the conditions applied in the present work. Some unsaturated ringlike hydrocarbon complexes can, however, appear in the irradiated HDT films, along with linear or chainlike atomic assemblies comprising C═C and C−C bonds.

5. Conclusion

Considering that a detailed knowledge of the electron irradiation induced damage in SAMs is of crucial importance for the optimization of the SAM-based lithography processes (and in particular low-energy electron lithography), we investigated the damage produced by low-energy electrons in hexadecanethiolate monolayers on gold substrates. HDT films were exposed to electrons of energies from 10 to 100 eV with doses between 30 and 14000 $\mu C/cm^2$. The irradiation-induced conformational and orientational damage, as well as changes of chemical bonding in the film, were monitored directly by infrared reflection−absorption spectroscopy, angle-resolved near edge X-ray absorption fine structure spectroscopy, and water drop contact angle measurements. The damage was found to occur immediately during the irradiation. The subsequent exposure of the irradiated films to air is believed to result in the appearance of COOH groups in the surface region presumably through chemical reactions of the irradiation-created free radicals with air oxygen.[20] The occurrence of such groups and a damage of hydrophobic terminal CH_3 groups leads to a significant raise of the hydrophilicity of the surface. This fact can be exploited in a wet chemical etching for pattern transfer into the substrate. The orientational and conformational disorder as well as the occurrence of irradiation-created free radicals in the bulk of the irradiated HDT film facilitates wetting of the etching solution and subsequent reaction with the metal substrate.

The obtained results are also of importance for the general understanding of the damage effects due to secondary electrons. Electrons of energies as low as 10 eV (typical for the secondary electrons) were found to be capable of damaging an alkanethiolate film. Therefore, damage effects due to the secondary electrons need to be considered in the experiments applying high-energy electron guns and X-ray sources. In the latter case special care should be taken to avoid sample exposure to the secondary electrons generated on the filament of an X-ray source, i.e., due to pinholes in the Al window typically used in X-ray sources.

The high sensitivity of HDT films to the electron irradiation with the primary energies as low as 10 eV can be also disadvantageous in some lithography applications. It was shown previously that in addition to the desired lithography structures artifacts are produced due to a reflection of secondary electrons in a strongly inhomogeneous electric field between an ultrasharp emitting tip and the substrate.[30]

Some problems remain to be studied in further work. First, the irradiation dose should be determined more accurately either through careful measurements of the energy-dependent secondary electron yield or through direct measurements of the primary electron current by a Faraday cup. Second, "in situ" NEXAFS measurements in an extended energy range are necessary to monitor the influence of the primary electron energy on irradiation-induced damage in detail. These measurements are also of importance to estimate possible effect of the primary energy on the predominate orientation of the C═C bonds in the irradiated sample. Additionally, a controlled, variable exposure of the irradiated samples to air (from several minutes to several days) is required to investigate probable slow reactions with an ambient atmosphere.

A very important question, which is also not addressed in the present investigation, is a possible influence of the electron irradiation on the sulfur headgroups in the alkanethiolate films. Previously disulfide formation has been observed after the irradiation of alkanethiolate monolayers on gold by Al Kα and Mg Kα X-ray sources.[29] Although this formation was related to damage caused by secondary electrons resulting from the photoemission process, there is no direct evidence that secondary electrons are really responsible for the observed changes. "in situ" photoelectron spectroscopy measurements on the S headgroups at progressive low-energy electron irradiation are necessary to come to an unambiguous conclusion.

Acknowledgment. We thank Dr. C. David and Prof. Ch. Wöll for valuable discussions and the BESSY staff, especially M. Mast, for technical help during some stages of the experiments. This work has been supported by the German Bundesministerium für Bildung, Wissenschaft, Forschung und Technologie (BMBF), through Grants 05 644 VHA 9 and 13N6186 as well as by the Fonds der Chemischen Industrie.

References and Notes

(1) Ulman, A. *An Introduction to Ultrathin Organic Films: Langmuir−Blodgett to Self- Assembly*, Academic Press: New York, 1991.
(2) Lee, T. R.; Laibinis, P. E.; Folkers, J. P.; Whitesides, G. M. *Pure Appl. Chem.* **1991**, *63*, 821.
(3) Stewart, K. R.; Whitesides, G. M.; Godfried, H. P.; Silvera, I. F. *Surf. Sci.* **1986**, *57*, 1381.
(4) Ulman, A. *J. Mater. Ed.* **1989**, *11*, 205.
(5) Hild, R.; David, C.; Müller, H. U.; Völkel, B.; Kayser, D. R.; Grunze, M. *Langmuir* **1998**, *14*, 342.
(6) Sagiv, J. *J. Am. Chem. Soc.* **1980**, *102*, 92.
(7) Sheen, C. W.; Shi, J.-X.; Martensson, J.; Parikh, A. N.; Allara, D. L. *J. Am. Chem. Soc.* **1992**, *114*, 1514.
(8) Tiberio, R. C.; Craighead, H. G.; Lercel, M. J.; Lau, T.; Sheen, C. W.; Allara, D. L. *Appl. Phys. Lett.* **1993**, *62*, 476.
(9) Lercel, M. J.; Tiberio, R. C.; Chapman, P. F.; Craighead, H. G.; Sheen, C. W.; Parikh, A. N.; Allara, D. L. *J. Vac. Sci. Technol.* **1993**, *B11*, 2823.
(10) Lercel, M. J.; Redinbo, G. F.; Pardo, F. D.; Rooks, M.; Tiberio, R. C.; Simpson, P.; Craighead, H. G.; Sheen, C. W.; Parikh, A. N.; Allara, D. L. *J. Vac. Sci. Technol.* **1994**, *B12*, 3663.
(11) Lercel, M. J.; Redinbo, G. F.; Rooks, M.; Tiberio, R. C.; Craighead, H. G.; Sheen, C. W.; Allara, D. L. *Microelectron. Eng.* **1995**, *27*, 43.
(12) Lercel, M. J.; Rooks, M.; Tiberio, R. C.; Craighead, H. G.; Sheen, C. W.; Parikh, A. N.; Allara, D. L. *J. Vac. Sci. Technol.* **1995**, *B13*, 1139.
(13) Müller, H. U.; David, C.; Völkel, B; Grunze, M. *J. Vac. Sci. Technol.* **1995**, *B13*, 2846.
(14) David, C.; Müller, H. U.; Völkel, B.; Grunze, M. *Microelectron. Eng.* **1996**, *30*, 57.
(15) Lercel, M. J.; Craighead, H. G.; Parikh, A. N.; Seshadri, K.; Allara, D. L. *Appl. Phys. Lett.* **1996**, *68*, 1504.
(16) Laibinis, P. E.; Graham, R. L.; Biebuyck, H. A.; Whitesides, G. M. *Science* **1991**, *254*, 981.
(17) Rieke, P. C.; Baer, D. R.; Fryxell, G. E.; Engelhard, M. H.; Porter, M. S. *J. Vac. Sci. Technol.* **1993**, *A11*, 2292.
(18) Baer, D. R.; Engelhard, M. H.; Schulte, D. W.; Guenther, D. E.; Wang, Li-Qiong; Rieke, P. C. *J. Vac. Sci.* **1994**, *A12*, 2478.
(19) Rowntree, P.; Dugal, P.-C.; Hunting, D.; Sanche, L. *J. Phys. Chem.* **1996**, *100*, 4546.
(20) Seshadri, K.; Froyd, K.; Parikh, A. N.; Allara, D. L.; Lercel, M. J.; Craighead, H. G. *J. Phys. Chem.* **1996**, *100*, 15900.
(21) Czanderna, A. W.; Jung, D. R. *Crit. Rev. Solid State. Mater. Sci.* **1994**, *19*, 1.
(22) Chidsey, C. E. D.; Liu, G.; Rowntree, P.; Scoles, G. *J. Chem. Phys.* **1989**, *91*, 4421.
(23) Poirier, G. E.; Tarlov, M. J. *Langmuir* **1994**, *10*, 2853.
(24) Nuzzo, R. G.; Korenic, E. M.; Dubois, L. H. *J. Chem. Phys.* **1990**, *93*, 767.
(25) Camillone, N.; Chidsey, C. E. D.; Liu, G.; Scoles, G. *J. Chem. Phys.* **1993**, *98*, 3503.
(26) Fenter, P.; Eberhardt, A.; Eisenberger, P. *Science* **1994**, *266*, 1216.
(27) Pertsin, A. J.; Grunze, M. *Langmuir* **1994**, *10*, 3668.
(28) Hähner, G.; Kinzler, M.; Thümmler, C.; Wöll, Ch.; Grunze, M. *J. Vac. Sci. Technol.* **1992**, *10*, 2758.
(29) Jäger, B.; Schürmann, H.; Müller, H. U.; Himmel, H.-J.; Neumann, M.; Grunze, M.; Wöll, Ch. *Z. Phys. Chem.* **1997**, *202*, 263.
(30) Völkel, B.; Gölzhäuser, A.; Müller, H. U.; David, C.; Grunze, M. *J. Vac. Sci. Technol.* **1997**, *B15*, 2877.
(31) Strong, L.; Whitesides, G. M. *Langmuir* **1988**, *4*, 546.
(32) Schaible, M.; Petersen, H.; Braun, W.; Koch, E. E. *Rev. Sci. Instrum.* **1989**, *60*, 2172.
(33) Bernstorff, S.; Braun, W.; Mast, M.; Peatman, W.; Schröder, T. *Rev. Sci. Instrum.* **1989**, *60*, 2097.
(34) Batson, P. E. *Phys. Rev. B* **1993**, *48*, 2608.

(35) Müller, H. U. Ph.D. Thesis, University Heidelberg, 1996.
(36) Petry, R. L. *Phys. Rev.* **1926**, *28*, 362.
(37) Kollath, R. In *Handbuch der Physik*; Flügge, S., Ed.; Springer-Verlag: New York, 1956; Vol. XXI, p 265.
(38) Dierscheke, P. Ph.D. Thesis, University Essen, 1988.
(39) Reimer, L.; Pfefferkorn, G. *Rasterelektronenmikroskopie*, Springer-Verlag: Berlin, 1977.
(40) Laibinis, P. E.; Whitesides, G. M.; Allara, D. L.; Tao, Y.-T.; Parikh, A. N.; Nuzzo, R. G. *J. Am. Chem. Soc.* **1991**, *113*, 7152.
(41) Stöhr, J. *NEXAFS Spectroscopy*; Springer Series in Surface Science 25; Springer-Verlag: Berlin, 1992.
(42) Bagus, P. S.; Weiss, K.; Schertel, A.; Wöll, Ch.; Braun, W.; Hellwig, H.; Jung, C. *Chem. Phys. Lett.* **1996**, *248*, 129.
(43) Schertel, A.; Hähner, G.; Grunze, M.; Wöll, Ch. *J. Vac. Sci. Technol.* **1996**, *A14*, 1801.
(44) Kinzler, M.; Schertel, A.; Hähner, G.; Wöll, Ch.; Grunze, M.; Albrecht, H.; Holzhüter, G.; Gerber, Th. *J. Chem. Phys.* **1994**, *100*, 7722.
(45) Nuzzo, R. G.; Korenic, E. M.; Dubois, L. H. *J. Chem. Phys.* **1993**, *93*, 767.
(46) Hähner, G.; Wöll, Ch.; Buck, M.; Grunze, M. *Langmuir* **1993**, *9*, 1955.
(47) Hähner, G.; Marti, A.; Spencer, N.; Brunner, S.; Caseri, W. R.; Suter, U. W.; Rehahn, M. *Langmuir* **1996**, *12*, 719.
(48) Bain, C. D.; Evall, J.; Whitesides, G. M. *J. Am. Chem. Soc.* **1989**, *111*, 7155.
(49) Holmes-Farley, S. R.; Whitesides, G. M. *Langmuir* **1987**, *3*, 62.
(50) Ashley, J. C. *Radiat. Res.* **1982**, *90*, 433.
(51) Atre, S. V.; Liedberg, B.; Allara, D. L. *Langmuir* **1995**, *11*, 3882.
(52) Rowntree, P.; Paranteau, L.; Sanche, L. *J. Phys. Chem.* **1991**, *95*, 4902.